View metadata, citation and similar papers at core.ac.uk
brought to you by CORE
provided by Elsevier - Publisher Connector

FEBS Letters 586 (2012) 1439–1444

FEBS Letters
journal homepage: www.FEBSLetters.org

Active site phosphoryl groups in the biphosphorylated phosphotransferase complex reveal dynamics in a millisecond time scale

Tae-Kyung Yu, Young-Joo Yun, Ko On Lee, Kyung Jun Ahn, Jeong-Yong Suh *

WCU Biomodulation Major, Department of Agricultural Biotechnology, Seoul National University, 599 Gwanak-ro, Gwanak-gu, Seoul 151-921, Republic of Korea

ARTICLE INFO

Article history:
Received 12 March 2012
Revised 10 April 2012
Accepted 12 April 2012
Available online 21 April 2012

Edited by Judit Ovádi

Keywords:
Biphosphorylated complex
Conformational exchange
NMR
Phosphotransferase system

ABSTRACT

The N-terminal domain of Enzyme I (EIN) and phosphocarrier HPr can form a biphosphorylated complex when they are both phosphorylated by excess cellular phosphoenolpyruvate. Here we show that the electrostatic repulsion between the phosphoryl groups in the biphosphorylated complex results in characteristic dynamics at the active site in a millisecond time scale. The dynamics is localized to phospho-His15 and the stabilizing backbone amide groups of HPr, and does not impact on the phospho-His189 of EIN. The dynamics occurs with the k_{ex} of ~500 s^{-1} which compares to the phosphoryl transfer rate of ~850 s^{-1} between EIN and HPr. The conformational dynamics in HPr may be important for its phosphotransfer reactions with multiple partner proteins.

Structured summary of protein interactions:
EIN and **HPr** bind by nuclear magnetic resonance (View Interaction).

© 2012 Federation of European Biochemical Societies. Published by Elsevier B.V. All rights reserved.

1. Introduction

The bacterial phosphotransferase system (PTS) catalyzes a series of phosphotransfer reactions coupled with sugar transport across the membrane [1,2]. Enzyme I and HPr form the first phosphotransfer protein complex in PTS, where the phosphoryl group is transferred from the active site His189 of Enzyme I to His15 of HPr in a reversible manner [3–5]. Enzyme I comprises an N-terminal domain (EIN) which is responsible for the phosphotransfer reaction with HPr, and a C-terminal domain which binds to phosphoenolpyruvate (PEP) for the auto-phosphorylation reaction. HPr relays the phosphoryl group from Enzyme I to sugar-specific membrane transporters, Enzymes II, which translocate and phosphorylate their sugar substrates [6].

The phosphorylation states of PTS proteins modulate their cellular protein–protein interactions and regulate gene expression for sugar metabolism and chemotaxis [5]. In the absence of external sugar substrates, high phosphotransfer potential of PEP keeps cellular PTS proteins in fully phosphorylated states [7,8]. The phosphorylated PTS proteins can still associate with each other to form a transient biphosphorylated complex, which possibly helps the PTS proteins to rapidly respond to the changes in the phosphorylation states of one another. We have recently reported the structure and the binding thermodynamics of the biphosphorylated complex between EIN and HPr [9]. We found that the biphosphorylated complex maintained the same backbone fold and binding interfaces as the unphosphorylated complex structure previously determined by NMR spectroscopy albeit with reduced affinity. The structure of the unphosphorylated complex can easily accommodate a phosphoryl group between the two active site histidine side chains to accomplish the phosphotransfer reaction [10]. In other words, placing two phosphoryl groups in the active site would cause a large electrostatic repulsion in the biphosphorylated complex. In this report, we examined how the active site of the biphosphorylated complex could accommodate two phosphoryl groups in close proximity. We show that the electrostatic repulsion is relieved by local dynamics at the active site of HPr at a millisecond time scale that is comparable to the phosphoryl transfer rate between EIN and HPr.

2. Materials and methods

2.1. Cloning, protein expression and purification

EIN and HPr were cloned into a pET11a vector without tags, and overexpressed in either Luria Bertini or minimal media with $^{15}NH_4Cl$ as the sole nitrogen source. Proteins were purified by DEAE anion exchange, G75 size exclusion, and monoQ anion exchange chromatography using an AKTA purification system (GE Healthcare) as previously described [9]. The fractions containing EIN or HPr were pooled and finally exchanged into the NMR buffer (20 mM Tris, pH 7.4).

* Corresponding author. Fax: +82 2 877 4906.
E-mail address: jysuh@snu.ac.kr (J.-Y. Suh).

0014-5793/$36.00 © 2012 Federation of European Biochemical Societies. Published by Elsevier B.V. All rights reserved.
http://dx.doi.org/10.1016/j.febslet.2012.04.020

2.2. NMR spectroscopy

NMR samples contained 1 mM EIN or HPr in 20 mM Tris, pH 7.4. HPr was phosphorylated using 50 mM PEP, 5 mM $MgCl_2$, and 10 μM Enzyme I. To phosphorylate EIN, 10 μM HPr was used in addition as Enzyme I did not directly phosphorylate EIN. ^{31}P NMR spectra were obtained using an *x,y,z*-shielded gradient quadruple resonance probe at 30 °C. $^{1}H–^{15}N$ correlation spectra were collected using Bruker Avance 600 MHz NMR spectrometer equipped with *z*-shielded gradient triple resonance cryoprobe at 37 °C. Long-range $^{1}H–^{15}N$ heteronuclear single quantum correlation (HSQC) spectra to monitor the imidazole side chains of histidines were recorded with a 22-ms dephasing delay. Titration experiments were carried out as follows: 1 mM phosphorylated HPr was prepared using 50 mM PEP, 5 mM $MgCl_2$, and 10 μM Enzyme I. Then phosphorylated EIN was added into phosphorylated HPr in a stoichiometric manner. Titration of unphosphorylated HPr was carried out in a similar manner except for the absence of PEP. NMR data were processed using the NMRPipe program and analyzed using the NMRView program [11,12].

3. Results

3.1. Model of the active site of the biphosphorylated complex

To estimate how close the two phosphoryl groups would be apart in the biphosphorylated complex, we first modeled the active site structure of the biphosphorylated EIN–HPr complex. The solution structure of an unphosphorylated EIN–HPr complex has been previously determined by NMR, and the active site is shown in Fig. 1A [10]. The active site His189 of EIN accepts a phosphoryl group at its Nε2 atom which is buried in the unphosphorylated state. Phosphorylation of EIN requires a change in the side chain χ_2 angle of His189 from g^+ to g^- conformation to expose the Nε2 atom to solvent to accommodate the incoming phosphoryl group [13]. In this conformation, Nε2 of His189 from and Nδ1 of His15 from HPr are brought together so that minimal structural displacement at the active site can easily accomplish successful phosphotransfer reactions. When we added two phosphoryl groups to the active site of the complex in this conformation, the distance between Nε2 atom of His189 of EIN and Nδ1 atom of His15 of HPr was measured as ~6.9 Å, and the distance between two phosphorus atoms was ~5.9 Å (Fig. 1B). Considering that there are two negative charges on each phosphoryl group at pH 7.4, large electrostatic repulsion is anticipated between the neighboring phosphoryl groups at the active site. To examine whether the electrostatic repulsion causes one or both of the phosphoryl groups to move away from each other, we first monitored the chemical shift change of the phosphoryl groups upon complex formation using ^{31}P NMR spectroscopy.

3.2. Chemical shift changes of phosphoryl groups from ^{31}P NMR

We used ^{31}P NMR to directly monitor the phosphoryl groups at the active site before and after the complex formation. Figs. 2A and 2B show the ^{31}P NMR spectra of phosphorylated EIN and HPr. The ^{31}P NMR signals at 2.02 ppm and −1.16 ppm originate from inorganic phosphate and PEP, respectively, at pH 7.4 and 30 °C (referenced to phosphoric acid at 0 ppm). The ^{31}P NMR signal of Nδ1-phosphorylated HPr appeared at −3.77 ppm, and that of Nε2-phosphorylated EIN appeared at −5.15 ppm. When the biphosphorylated complex was formed, the ^{31}P NMR signal of the phosphorylated HPr split into two peaks at −3.13 ppm and −4.68 ppm, with significant line-broadening (Fig. 2C). This is characteristic of an

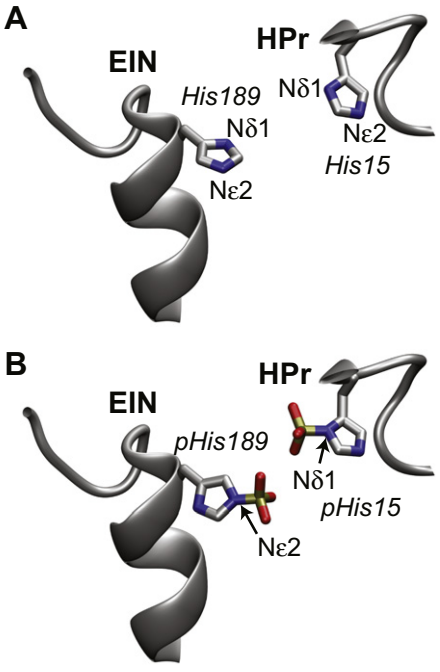

Fig. 1. (A) The three-dimensional structure of the active site of the unphosphorylated complex between EIN and HPr determined by NMR spectroscopy (PDB code: 3EZA), [10] and (B) a model structure of the active site of the biphosphorylated complex. Only the side chains of active site His189 in EIN and His15 in HPr were drawn in stick model. The side-chain atoms are *color-coded* according to atom types: carbon (*gray*), nitrogen (*blue*), oxygen (*red*), and phosphorus (*yellow*).

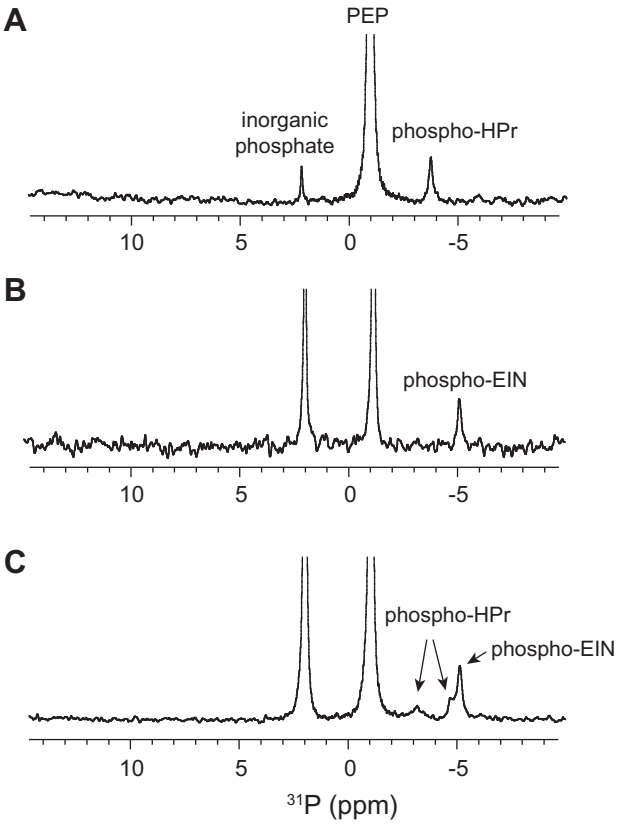

Fig. 2. ^{31}P NMR spectra of (A) 1 mM of phosphorylated HPr, (B) 1 mM of phosphorylated EIN, and (C) 1 mM of phosphorylated HPr with 1 mM of phosphorylated EIN. 10 μM of Enzyme I, 5 mM $MgCl_2$ as well as 50 mM PEP were used to keep the HPr and EIN in fully phosphorylated states during the measurement.

exchange rate on the slow side of intermediate exchange, where $\Delta\omega_P \sim 2400\ s^{-1}$ suggests that the exchange occurs at $\sim 500\ s^{-1}$ ($5k_{ex} \sim \Delta\omega_P$). We will show that the similar exchange rates are observed from backbone and side chain ^{15}N nuclei of HPr using $^{1}H–^{15}N$ correlation spectroscopy in the following sections.

We exclude the possibility that the change of ^{31}P NMR signal of phospho-HPr results from the loss of phosphoryl group of HPr in the complex. The phosphorylation state of EIN and HPr can be unambiguously determined from their signature chemical shift patterns upon phosphorylation in the $^{1}H–^{15}N$ HSQC spectra. We examined the $^{1}H–^{15}N$ HSQC spectra of the biphosphorylated complex before and after the ^{31}P NMR measurement, and EIN and HPr were both in fully phosphorylated states in the complex. Also, the loss of the phosphoryl group on the histidine to buffer by acid-catalyzed hydrolysis is slow on the chemical shift time scale with the half-life of the phosphohistidine as ~20 min [9,14]. Hence, the hydrolysis of the phosphoryl group and the subsequent phosphotransfer reaction between EIN and HPr cannot contribute to the observed line-broadening.

We note that the ^{31}P NMR signal of the phosphorylated EIN remained the same regardless of the complex formation. The result indicates that observed dynamics is localized at the active site phosphoryl group on HPr, and does not impact on the phosphoryl group on EIN. This is unexpected since the phosphoryl group on HPr is stabilized by hydrogen bonds to the backbone amides of Thr16 and Arg17, both of which form the secondary structure of the α-helix in HPr [15]. On the other hand, the phosphoryl group on EIN is exposed to solvent, with a hydrogen bond to the side chain Lys69. We used $^{1}H–^{15}N$ NMR to further examine the change of the side chain imidazole group of His15 and the backbone amide groups of Thr16 and Arg17 in HPr.

3.3. Side chain imidazole of the active site in the biphosphorylated complex

The tautomerism and protonation states of the imidazole group of a histidine can be conveniently identified by long-range $^{1}H–^{15}N$ HSQC spectroscopy [16]. The imidazole side chain of a histidine adopts either an Nε2-H tautomer or an Nδ1-H tautomer in neutral and basic solution, where the Nε2-H tautomer is generally a more stable form [17]. The tautomeric state of the active site His189 of EIN has been well characterized in the unphosphorylated and the phosphorylated states [13,18]. Here we briefly describe the tautomeric and protonation states of the active site His15 of HPr before and after phosphorylation, and then compare the chemical shift perturbation when HPr is titrated by EIN.

Fig. 3A shows the long-range $^{1}H–^{15}N$ HSQC of HPr in its unphosphorylated (black) and phosphorylated (red) states. ^{15}N chemical shifts of the imidazole ring of histidine range from ~168 ppm of a proton-attached nitrogen nucleus to ~250 ppm of a proton-removed nitrogen nucleus [19]. Also, ^{15}N chemical shifts are affected by protonation, so that both nitrogen nuclei resonate around 180 ppm when the imidazole ring is fully protonated and positively charged [19]. When HPr is unphosphorylated, both His15 and His76 appear as Nε2-H tautomeric states, which agrees with previous 1D ^{15}N NMR data [20]. Nδ1 of the active site His15 resonates at 238.6 ppm and Nε2 resonates at 173.9 ppm in unphosphorylated HPr, which indicates an Nε2-H tautomer in a neutral form. When HPr is phosphorylated, His15 makes a significant change in the chemical shifts and Nδ1 and Nε2 resonate at 206.6 ppm and at 194.4 ppm, respectively. From studies of N-phosphoimidazole and phosphomethylimidazole compounds, phosphorus-attached ^{15}N resonates at 202 ppm in a neutral state and at 210 ppm in a protonated state [19]. The phosphorus-unattached ^{15}N of the phosphoimidazole resonates at 244 ppm in a neutral state and 174 ppm in a protonated state. The ^{15}N chemical shifts of phosphorylated HPr

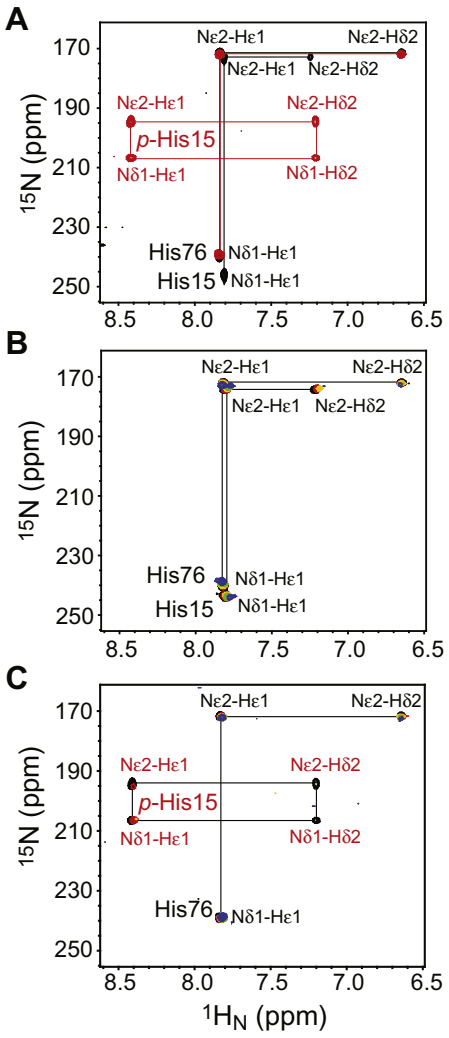

Fig. 3. Long-range $^{1}H–^{15}N$ HSQC spectra of (A) unphosphorylated (*black*) and phosphorylated (*red*) ^{15}N-labeled HPr, (B) unphosphorylated ^{15}N-labeled HPr titrated by EIN, and (C) phosphorylated ^{15}N-labeled HPr titrated by phosphorylated EIN. The molar ratios in the titration spectra are *color-coded* as follows: 0 (*black*), 0.1 (*red*), 0.2 (*yellow*), 0.3 (*green*), 0.5 (*blue*). The spectra were recorded with a 22 ms dephasing delay for the ^{1}H and ^{15}N signals to become antiphase. In EIN spectra, only the cross-peaks of the active site His189 are annotated for simplicity.

are consistent with the Nδ1 phosphorylation of His15 and indicate that the imidazole ring is partly protonated. Chemical shifts of His76 little changed by the phosphorylation reaction, and maintained the Nε2-H tautomeric state.

We then monitored the long-range $^{1}H–^{15}N$ HSQC of ^{15}N-labeled HPr titrated by EIN both in unphosphorylated or phosphorylated states in Figs. 3B and 3C. When HPr binds to EIN in the unphosphorylated state, there were little changes in the chemical shifts of His15 and His76, though the cross-peaks experienced gradual decrease of peak intensity due to increased molecular weight by the complex formation. Note that the Nε2-Hδ2 cross-peaks are weaker due to the smaller scalar coupling [21], but Nε2-Hε1 and Nδ1-Hε1 cross-peaks can be clearly observed throughout the titration in Fig. 3B. The result indicates that His15 of HPr does not change its tautomeric state upon binding to EIN in the unphosphorylated state. It has previously been reported that His189 of unphosphorylated EIN does not change its tautomeric state upon binding to HPr as well [22]. Hence, both active site histidines of HPr and EIN keep their tautomeric states unchanged upon complex formation in the unphosphorylated state. On the other hand, when

Equation (1):

$$[H]_{bound} = \frac{([E]_T + [H]_T + K_D) - \sqrt{([E]_T + [H]_T + K_D)^2 - 4[E]_T[H]_T}}{2}$$

Equation (2):

$$\Delta\omega = \omega_{bound} - \omega_{free} = \frac{(\omega_{obs} - \omega_{free})[H]_T}{[H]_{bound}}$$

Fig. 4. Equation (1) is used to calculate the concentration of HPr in the bound state, where $[H]_{bound}$ is the concentration of HPr in the bound state, $[E]_T$ and $[H]_T$ are the total concentrations of EIN and HPr, respectively, and K_D is the equilibrium dissociation constant. Equation (2) is used to calculate the frequency difference between the free and bound states of HPr, where $\Delta\omega$ is the frequency difference between the free and bound states of HPr, ω_{bound} and ω_{free} are the chemical shifts of bound and free states, respectively, ω_{obs} is the observed chemical shift in the titration, and $[H]_T$ and $[H]_{bound}$ are the total HPr concentration and the HPr concentration in the bound state, respectively.

HPr was titrated with EIN in the phosphorylated state, the cross-peaks of phosphorylated His15 exhibited a significant line-broadening, indicating an intermediate exchange on the chemical shift time scale (Fig. 3C). The equilibrium dissociation constant (K_D) between HPr and EIN in their phosphorylated states have been reported as ~108 μM [9]. The concentration of HPr in the bound state, $[H]_{bound}$ can be calculated by the equation (1) in Fig. 4. The frequency difference between the free and bound states ($\Delta\omega$) of HPr is then obtained by the equation (2) in Fig. 4.

The $\Delta\omega$ for the Hε1 resonance of His15 is thus calculated as 550 s^{-1}, and the intermediate exchange indicates that the exchange rate constant k_{ex} is ~550 s^{-1} ($k_{ex} \sim \Delta\omega_H$). As the ^{15}N chemical shifts of the imidazole group of His15 did not indicate any change in the tautomeric or protonation states, the exchange likely originates from conformational dynamics of the imidazole group. The obtained k_{ex} of the side chain imidazole group is very close to the k_{ex} obtained from ^{31}P NMR spectra, suggesting that the two k_{ex} values report the same motion of the phosphorylated side chain of His15 of HPr. We note that the cross-peaks of His76 did not show such line-broadening during the titration in the phosphorylated state as well as in the unphosphorylated state.

3.4. Dynamics of backbone amide groups at the active site

We also monitored the chemical shift perturbation of backbone amide resonances of ^{15}N-HPr titrated by EIN in the phosphorylated state using the ^1H–^{15}N HSQC experiment. The residues with chemical shift perturbation from the titration in the phosphorylated state behaved very similarly as they did during the titration in the unphosphorylated states (See Fig. 1S in Supplementary data). The only exception was the active site region, where the backbone amide protons of His15, Thr16, and Arg17 exhibited a fast exchange during the titration in the unphosphorylated state (Fig. 5A and B), but they disappeared by line-broadening during the titration in the phosphorylated state (Fig. 5C and D). The complete line-broadening was observed only in the three residues, and the other residues with chemical shift perturbation exhibited a typical fast exchange on the chemical shift time scale. As previous study showed that the phosphoryl group on HPr15 is stabilized by hydrogen bonds to the backbone amide protons of Thr16 and Arg17, the observed line-broadening in the backbone amide groups could be linked to the motions of the side chain of phospho-His15 that we described in the previous sections [15].

We calculated the chemical shift differences of the backbone amide groups between free and bound states using the equations (1) and (2) in Fig. 4. The frequency difference ($\Delta\omega_N$) of His15 was obtained as ~500 s^{-1}, and the intermediate exchange suggests the exchange rate constant k_{ex} ~500 s^{-1}. The frequency difference of the backbone amide group of Thr16 was obtained as $\Delta\omega_H$ ~600 s^{-1}, and that of Arg17 was $\Delta\omega_N$ ~400 s^{-1}. Since the backbone

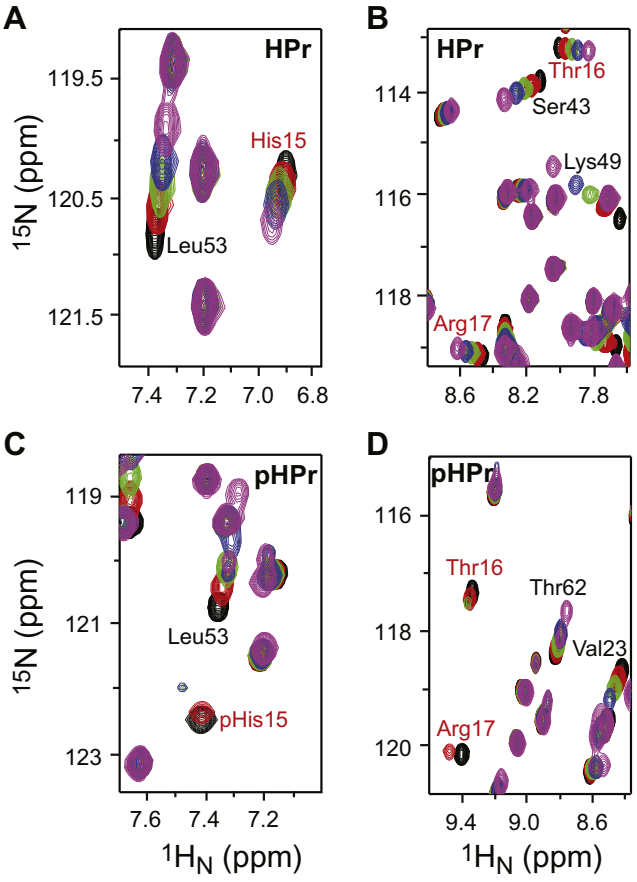

Fig. 5. Selected cross-peaks in the ^1H–^{15}N HSQC spectra during the titration of EIN into ^{15}N-labeled unphosphorylated HPr for (A) His15, and (B) Thr16 and Arg17, and the titration of phosphorylated EIN into ^{15}N-labeled phosphorylated HPr for (C) phosphorylated His15, and (D) Thr16 and Arg17. Note large chemical shift changes of His15, Thr16, and Arg17 upon phosphorylation. The molar ratios in the titration spectra are *color-coded* as follows: 0 (*black*), 0.1 (*red*), 0.2 (*green*), 0.3 (*blue*), 0.5 (*magenta*). His15, Thr16, and Arg17 were annotated in *red* for visual guidance.

amide resonances of Thr16 and Arg17 exhibited an intermediate exchange with complete line-broadening during the titration, the k_{ex} values for these two resonances correspond to 400–600 s^{-1}. From the titration of phosphorylated HPr with EIN, the amide group of Thr52 exhibited the largest chemical shift perturbation with $\Delta\omega_N$ ~3000 s^{-1}, which was in the fast exchange in the chemical shift time scale. As the exchange rate constant from the association and dissociation between HPr and EIN would be larger than 3000 s^{-1}, it cannot contribute to the observed line-broadening of the backbone amide groups. Thus, the k_{ex} values

obtained from the phosphoryl group, the imidazole side chain, and the backbone amide groups altogether report a motion of phospho-His15 that occurs at $\sim 500\ s^{-1}$. We suppose that the exchange of the backbone amides of Thr16 and Arg17 is caused by the formation and loss of hydrogen bonds due to the dynamics of the phosphoryl group on His15, since these backbone amide groups are in the α-helical secondary structure.

4. Discussion

The ^{31}P NMR study indicates that the phosphoryl group of HPr exchanges between two conformational states in the biphosphorylated complex. The exchange broadening of the backbone amides suggests that the conformational states are distinct in the hydrogen bonds between the phosphoryl group and the backbone amides. As the loop region between Ala10 and Leu14 preceding the active site His15 of HPr was little affected by the motion, we infer that the conformational change is highly localized to the active site, and the imidazole ring of His15 should stick out away from the loop region when it is not engaged in the hydrogen bonds. We do not have the detailed structural information on the conformational states, but it is notable that the dynamics of the phosphoryl groups in the biphosphorylated complex occurs at $\sim 500\ s^{-1}$, which compares to the phosphotransfer rate between EIN and HPr of $\sim 850\ s^{-1}$ from exchange spectroscopy [9]. We expect that the physical motions in the biphosphorylated complex and the phosphotransfer complex would be different: the former would direct to minimize the electrostatic repulsion between the phosphoryl groups, while the latter would appose the imidazole groups in order to accomplish the enzyme reaction. In this sense, the active site phospho-His15 of HPr explores distinct conformational states depending on the local environment at the interface of the complex. The multiple conformational states of HPr may be beneficial to its function, given that HPr interacts with the A domains of various Enzymes II (e.g. IIA^{Glc}, IIA^{Mtl}, IIA^{Mann}, IIA^{Chb}, etc.) as well as EIN [23–25]. HPr binds to multiple partner proteins that are unrelated in their sequences as well as in their structures using a common interaction interface, and achieves phosphotransfer reactions between the conserved active site histidine residues. Multiple conformational states available to the active site His15 of HPr may help to coordinate and fine-tune the phosphoryl transfer reactions in different protein complexes.

Electrostatic interactions in proteins are important in many aspects such as folding, structure and stability [26,27]. Electrostatic repulsion often results in dissociation of a protein complex or a conformational change [28–30], but can also be compromised by water molecules bridging with hydrogen bonds [31]. Our study illustrates an example in which electrostatic repulsion at the interaction interface of a protein complex can give rise to local dynamics that was unseen in the isolated individual proteins. In the biphosphorylated complex between EIN and HPr, the electrostatic repulsion at the interaction interface is not relieved by neutralizing side chains or water-bridged hydrogen bonds, but by local dynamic motions at the active site. Characterization of as many individual dynamic states in a given protein complex would enhance our understanding of protein dynamics and its functional implication.

Acknowledgements

This work was supported by WCU (World Class University) program (R31-10056), and National Research Foundation of Korea (NRF) grant funded by the Ministry of Education, Science and Technology (2011-0025901 and 2011-0027662). We thank the high field NMR facility at Korea Basic Science Institute for NMR experiments.

Appendix A. Supplementary data

Supplementary data associated with this article can be found, in the online version, at http://dx.doi.org/10.1016/j.febslet.2012.04.020.

References

[1] Kundig, W., Ghosh, S. and Roseman, S. (1964) Phosphate bound to histidine in a protein as an intermediate in a novel phosphor-transferase system. Proc. Natl. Acad. Sci. USA 52, 1067–1074.
[2] Postma, P.W., Lengeler, J.W. and Jacobson, G.R. (1993) Phosphoenolpyruvate: carbohydrate phosphotransferase systems of bacteria. Microbiol. Rev. 57, 543–594.
[3] Weigel, N., Kukuruzinska, M.A., Nakazawal, A., Waygoodll, E.B. and Roseman, S. (1982) Sugar transport by the bacterial phosphotransferase system. Phosphoryl transfer reactions catalyzed by Enzyme I *Salmonella typhimurium*. J. Biol. Chem. 257, 14477–14491.
[4] Weigel, N., Powers, D.A. and Roseman, S. (1982) Sugar transport by the bacterial phosphotransferase system. Primary structure and active site of a general phosphocarrier protein (HPr) from Salmonella typhimurium. J. Biol. Chem. 257, 14499–14509.
[5] Deutscher, J., Francke, C. and Postma, P.W. (2006) How phosphotransferase system-related protein phosphorylation regulates carbohydrate metabolism in bacteria. Microbiol. Mol. Biol. Rev. 70, 939–1031.
[6] Siebold, C., Flukiger, K., Beutler, R. and Erni, B. (2001) Carbohydrate transport of the bacterial phosphoenolpyruvate sugar phosphotransferase system (PTS). FEBS Lett. 504, 104–111.
[7] Tanaka, Y., Kimata, K. and Aiba, H. (2000) A novel regulatory role of glucose transporter of Escherichia coli: membrane sequestration of a global repressor Mlc. EMBO J. 19, 5344–5352.
[8] Nam, T.W., Cho, S.H., Shin, D., Kim, J.H., Jeong, J.Y., Lee, J.H., Roe, J.H., Peterkofsky, A., Kang, S.O., Ryu, S. and Seok, Y.J. (2001) The Escherichia coli glucose transporter enzyme $IICB^{Glc}$ recruits the global repressor Mlc. EMBO J. 20, 491–498.
[9] Suh, J.Y., Cai, M. and Clore, G.M. (2008) Impact of phosphorylation on structure and thermodynamics of the interaction between the N-terminal domain of Enzyme I and the histidine phosphocarrier protein of the bacterial phosphotransferase system. J. Biol. Chem. 283, 18980–18989.
[10] Garrett, D.S., Seok, Y.J., Peterkofsky, A., Gronenborn, A.M. and Clore, G.M. (1999) Solution structure of the 40,000 Mr phosphoryl transfer complex between the N-terminal domain of enzyme I and HPr. Nature Struct. Biol. 6, 166–173.
[11] Delaglio, F., Grzesiek, S., Vuister, G.W., Zhu, G., Pfeifer, J. and Bax, A. (1995) NMRPipe: A multidimensional spectral processing system based on UNIX pipes. J. Biomol. NMR 6, 277–293.
[12] Johnson, B.A. and Blevins, R.A. (1994) NMRView: A computer program for he visualization and analysis of NMR data. J. Biomol. NMR 4, 603–614.
[13] Garrett, D.S., Seok, Y.J., Peterkofsky, A., Clore, G.M. and Gronenborn, A.M. (1998) Tautomeric state and pK_a of the phosphorylated active site histidine in the N-terminal domain of enzyme I of the Escherichia coli phosphoeno1pyruvate:sugar phosphotransferase system. Protein Sci. 7, 789–793.
[14] Suh, J.Y., Iwahara, J. and Clore, G.M. (2007) Intramolecular domain-domain association/dissociation and phosphoryl transfer in the mannitol transporter of Escherichia coli are not coupled. Proc. Natl. Acad. Sci. USA 104, 3153–3158.
[15] Van Dijk, A.A., Scheek, R.M., Dijkstra, K., Wolters, G.K. and Robillard, G.T. (1992) Characterization of the protonation and hydrogen bonding state of the histidine residues in IIA^{mtl}, a domain of the phosphoenolpyruvate-dependent mannitol-specific transport protein. Biochemisty 31, 9063–9072.
[16] Reynolds, W.F., Peat, I.R., Freedman, M.H. and Lyerla Jr, J.R. (1973) Determination of the tautomeric form of the imidazole ring of L-histidine in basic solution by carbon-13 magnetic resonance spectroscopy. J. Am. Chem. Soc. 95, 328–331.
[17] Garrett, D.S., Seok, Y.J., Liao, D., Peterkofsky, A., Gronenborn, A.M. and Clore, G.M. (1997) Solution structure of the 30 kDa N-terminal domain of Enzyme I of the Escherichia coli phosphoenolpyruvate:sugar phosphotransferase system by multidimensional NMR. Biochemistry 36, 2517–2530.
[18] Pelton, J.G., Torchia, D.A., Meadow, N.D. and Roseman, S. (1993) Tautomeric states of the active-site histidines of phosphorylated and unphosphorylated III^{Glc}, a signal-transducing protein from Escherichia coli, using two-dimensional heteronuclear NMR techniques. Protein Sci. 2, 543–558.
[19] van Dijk, A.A., de Lange, L.C.M., Bachovchin, W.W. and Robillard, G.T. (1990) Effect of phosphorylation on hydrogen-bonding interactions of the active site histidine of the phosphocarrier protein HPr of the phosphoenolpyruvate-dependent phosphotransferase system determined by ^{15}N NMR spectroscopy. Biochemistry 29, 8164–8171.
[20] Blomberg, F., Maurer, W. and Ruterjans, H. (1977) Nuclear magnetic resonance investigation of ^{15}N-labeled histidine in aqueous solution. J. Am. Chem. Soc. 99, 8149–8159.
[21] Garrett, D.S., Seok, Y.J., Peterkofsky, A., Clore, G.M. and Gronenborn, A.M. (1997) Identification by NMR of the binding surface for the histidine-containing phosphocarrier protein HPr on the N-terminal domain of Enzyme I of the Escherichia coli phosphotransferase system. Biochemisty 36, 4393–4398.

[22] van Nuland, N.A.J., Boelens, R., Scheek, R.M. and Robillard, G.T. (1995) High-resolution structure of the phosphorylated form of the histidine-containing phosphocarrier protein HPr from Escherichia coli determined by restrained molecular dynamics from NMR-NOE data. J. Mol. Biol. 246, 180–193.
[23] Wang, G., Louis, J.M., Sondej, M., Seok, Y.J., Peterkofsky, A. and Clore, G.M. (2000) Solution structure of the phosphoryl transfer complex between the signal transducing proteins HPr and $IIA^{Glucose}$ of the *Escherichia coli* phosphoenolpyruvate:sugar phosphotransferase system. EMBO J. 19, 5635–5649.
[24] Suh, J.Y., Cai, M., Williams Jr., D.C. and Clore, G.M. (2006) Solution structure of a post-transition State analog of the phosphotransfer reaction between the A and B cytoplasmic domains of the mannitol transporter II mannitol of the *Escherichia coli* phosphotransferase system. J. Biol. Chem. 281, 8939–8949.
[25] Williams Jr., D.C., Cai, M., Suh, J.Y., Peterkofsky, A. and Clore, G.M. (2005) Solution NMR structure of the 48-kDa IIAMannose–HPr complex of the *Escherichia coli* mannose phosphotransferase system. J. Biol. Chem. 280, 20775–20784.
[26] Perutz, M.F. (1978) Electrostatic effects in proteins. Science 201, 1187–1191.
[27] Horovitz, A., Serrano, L., Avron, B., Bycroft, M. and Fersht, A.R. (1990) Strength and co-operativity of contributions of surface salt bridges to protein stability. J. Mol. Biol. 216, 1031–1044.
[28] Lunelli, L., Bucci, E. and Baldini, G. (1993) Electrostatic interactions in hemoglobin from light scattering experiments. Phys. Rev. Lett. 70, 513–516.
[29] Dodson, G.G., Lane, D.P. and Verma, C.S. (2008) Molecular simulations of protein dynamics: new windows on mechanisms in biology. EMBO Rep. 9, 144–150.
[30] Querfurth, C., Diernfellner, A.C.R., Gin, E., Malzahn, E., Hofer, T. and Brunner, M. (2011) Circadian conformational change of the neurospora clock protein frequency triggered by clustered hyperphosphorylation of a basic domain. Mol. Cell. 43, 713–722.
[31] Magalhaes, A., Maigret, B., Hoflack, J., Gomes, J.N.F. and Scheraga, H.A. (1994) Contribution of unusual arginine-arginine short-range interactions to stabilization and recognition in proteins. J. Prot. Chem. 13, 195–215.